Kinetic Analysis of Copper(I)/Feringa-Phosphoramidite Catalysed $AlEt_3$ 1,4-Addition to Cyclohex-2-en-1-one

Darren Willcox,† Ryan Nouch,† Alexander Kingsbury,† David Robinson,‡ Joe V. Carey,§ Steve Brough,§ Simon Woodward,†*

†GSK Carbon Neutral Laboratories for Sustainable Chemistry, University of Nottingham, Jubilee Campus, Nottingham NG7 2TU, United Kingdom
‡Department of Chemistry and Forensics, School of Science and Technology, Nottingham Trent University, Clifton Lane, Nottingham NG11 8NS, United Kingdom
§Key Organics Ltd, Highfield Road Industrial Estate, Camelford, Cornwall PL32 9RA, United Kingdom

ABSTRACT: ReactIR studies of mixtures of $AlEt_3$ (**A**) and cyclohex-2-en-1-one (**CX**) in Et_2O indicate immediate formation of the Lewis acid-base complex (**CX.A**) at -40 °C (K = 12.0 M^{-1}, ΔG^{o}_{react} -1.1 kcal mol^{-1}). Copper(I) catalysts, derived from pre-catalytic $Cu(OAc)_2$ (up to 5 mol-%) and (*R,S,S*)-P(binaphtholate){N(CHMePh)$_2$} [Feringa's ligand (**L**), up to 5 mol-%] convert **CX.A** (0.04-0.3 M) into its 1,4-addition product enolate (**E**) within 2000 sec at -40 °C. Kinetic studies (ReactIR and chiral GC) of **CX.A**, **CX** and (*R*)-3-ethylcyclohexanone (**P**, the H^+ quench product of enolate **E**) show that the true catalyst is formed in the first 300 sec and this subsequently provides **P** in 82% *ee*. This true catalyst converts **CX.A** to **E** with a rate law $[Cu]^{1.5}[\mathbf{L}]^{0.66}[\mathbf{CX.A}]^{1}$ when [**L**]/[Cu] ≤ 3.5. Above this ligand ratio inhibition by added ligand with order $[\mathbf{L}]^{-2.5}$ is observed. A rate determining step (rds) of $Cu_3\mathbf{L}_2(\mathbf{CX.A})_2$ stoichiometry is shown to be most consistent with the rate law. The presence of the enolate in the active catalyst (Graphical Abstract) best accounts for the reaction's induction period and molecularity as [**E**] ≡ [**CX.A**]. Catalysis proceeds through a 'shuttling mechanism' between two C_2 symmetry related ground state intermediates. Each turnover consumes one equivalent of **CX.A**, expels one molecule of **E** and forms the new Cu-Et bond needed for the next cycle (Graphic Abstract). The observed ligand (**L**) inhibition and a non-linear ligand **L***ee* effect on the *ee* of **P** are all well simulated by the kinetic model. DFT studies [ωB97X-D/SRSC] support coordination of **CX.A** to the groundstate Cu-trimer and its rapid conversion to **E**.

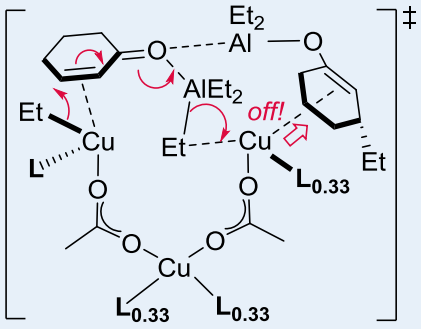

KEYWORDS: *conjugate addition, mechanism, asymmetric, aluminum, copper, density functional theory*

■ INTRODUCTION

Copper-catalysed conjugate (1,4-)additions of alkyl organometallic reagents to Michael acceptors have become 'go to' methods for enantioselective C–C bond construction, due to their reliability and often exceptional (frequently 90-95% *ee*) selectivities.[1] Typically, organozinc and Grignard reagents are employed as the terminal alkyl (R^-) source with a wide range of *in situ* formed copper(I) catalysts using diverse chiral ligands (L) including: phosphines, *N*-heterocyclic carbenes (NHCs) and, especially, phosphoramidites.[2] The consensus mechanistic view of these 1,4-additions to enones (and related Michael acceptors), catalysed by 'RCuL_n', is given in Scheme 1.[3] Rapid reduction by MR (e.g. RMgX, ZnR_2) of copper(II) pre-catalysts means that only catalytic cycles starting from Cu^{I} operate. Initial π-complexes **1**[4] are thought to undergo oxidative addition to σ-alkyl Cu^{III} complexes **2**.[5] The reductive elimination step is thought to be the stereo-determining turnover limiting step and this has been proposed to be strongly accelerated by coordination of π-acceptor ligands to the σ-Cu^{III} intermediate providing enolates **3**.[1-3] The organocopper byproduct is then re-cycled to **1** to restart the catalytic cycle. The role of the bridging ligand (X) is to arrange the hard (M) and soft (Cu^{I}) Lewis acidic sites to provide dual activation for the Michael acceptor, both halides and pseudohalides have been used in this role.

Hard evidence (as opposed to mechanistic conjecture) supporting the intimate details of the transition states providing such cycles is limited but has been described for Grignard additions (e.g. the structure of **4** has been deduced through kinetic and NMR studies of isolable model complexes of the reaction intermediates).[6] On the basis of kinetic studies transition state **5** was proposed for ACA reactions of $ZnEt_2$;[7] it is essentially a transposition of Noyori's proposal for 1,4-$ZnEt_2$ addition (from an earlier kinetic study of achiral sulphonamide catalysts[8]) but with an added chiral ligand. Through intensive NMR studies of CuX/**L** model systems (mostly in CD_2Cl_2) Gschwind[9] and co-workers proposed the hypothesis that the dominant transition state in 'real' catalytic systems adding $ZnEt_2$ to cyclohex-2-en-1-one must be **6**.

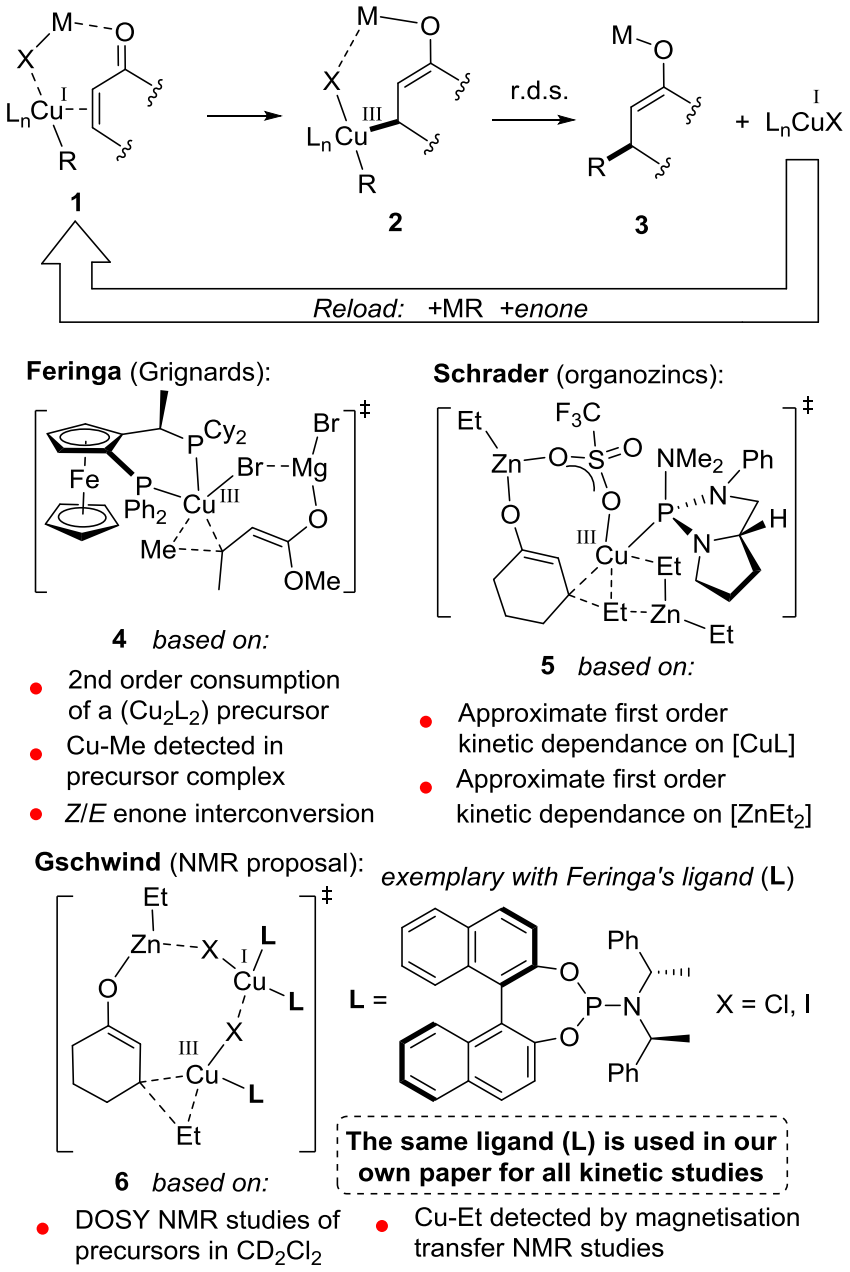

Scheme 1. Contemporary understanding of the mechanism of catalytic Asymmetric Conjugate Addition (ACA) and a summary of evidences cited to support such proposals. Throughout this present paper (*R*,*S*,*S*)-Feringa's ligand (**L**) above is used for all studies.

In the last decade the use of organoalanes (AlR_3) has become a popular modern variant for ACA reactions.[10] Very reactive catalytic systems are realised allowing even for the formation of chiral quaternary centres by addition to β,β-disubstituted Michael acceptors.[1,11] Surprisingly, very little is known[12] about the critical transition state responsible for catalyst turnover in copper-promoted 1,4-additions of AlR_3 to enones, despite their common usage in the synthetic community.[10]

Gschwind's proposal that speciation in ACA reactions is dominated by a single entity[9] suggests that classical reaction kinetics might be an effective way of estimating the composition of the $AlR_3/Cu^I/L$ active specie (e.g. Cu_xL_y etc.) through reaction component order analysis. This prompted us to undertake a kinetic study of the model transformation of Scheme 2, based on a mixture of cyclohex-2-en-1-one (cyclohexenone, **CX**) and $AlEt_3$ (**A**) catalysed by pre-catalytic $Cu(OAc)_2$ (**Cu**) in the presence of the optimal (*R,S,S*)-Feringa's ligand (**L**, structure in Scheme 1). On workup the initially formed enolate (**E**) is converted to the enantioenriched ketone product (**P**).

Scheme 2. Model system studied in this publication: cyclohex-2-en-1-one (**CX**), $AlEt_3$ (**A**), $Cu(OAc)_2$ [and its derived copper(I) reduction product] (**Cu**) and (*R,S,S*)-Feringa's ligand (**L**). This leads to the formation of the (*R*)-enolate (**E**), and on its hydrolysis, the (*R*)-ketone product (**P**).

■ RESULTS

Formation of a CX.A adduct. Mixing cyclohex-2-en-1-one (**CX**) and $AlEt_3$ (**A**) at -40 °C in Et_2O instantaneously gives a bright yellow solution that is stable for at least 30 mins under these conditions. After aqueous quench (2 M, aq. HCl), **CX** is recovered quantitatively, indicating no uncatalysed 1,4-addition takes place under these conditions and that all other irreversible uncatalysed processes are also negligible. The nature of the bright yellow reactive intermediate was investigated by ReactIR monitored titration of **A** into **CX** (Runs 1-2, Supporting Information). The intensity of the carbonyl stretching signal of **CX** (1676 cm^{-1}) falls after addition of each **A** aliquot as a new species with ν(C=O) 1630 cm^{-1} grows in (Figure 1). Variation of the **CX**:**A** stoichiometry indicates the 1:1 Lewis acid-base complex **CX.A** is formed.[13,14] Fitting the appropriate reaction isotherm (Supporting Information, Runs 1-2) gives an association constant K = 12.0(8) M^{-1} between **A** and **CX**, corresponding to a ΔG^{o}_{react} of -1.1 kcal mol^{-1} at -40 °C. Based on the calculated **CX** and **CX.A** concentrations (between 129-481 and 3-207 mM respectively) the molar constants were determined as ε_{CX} = 0.565 M and $\varepsilon_{CX.A}$ = 0.697 M. In order to attain accurate absolute quantification of [**CX.A**] careful zero calibration of the ReactIR setup is required. The calculated ΔΔG(-40 °C) difference between the related, experimentally determined, $MeAl(BHT)_2(O{=}CPh_2)$ and $MeAl(BHT)_2(OEt_2)$ [BHT = 2,6-di-*tert*-butyl-4-methylphenolate] using the figures of Power[13] is similar at ΔG^{o}_{react} = -1.45 kcal mol^{-1}.

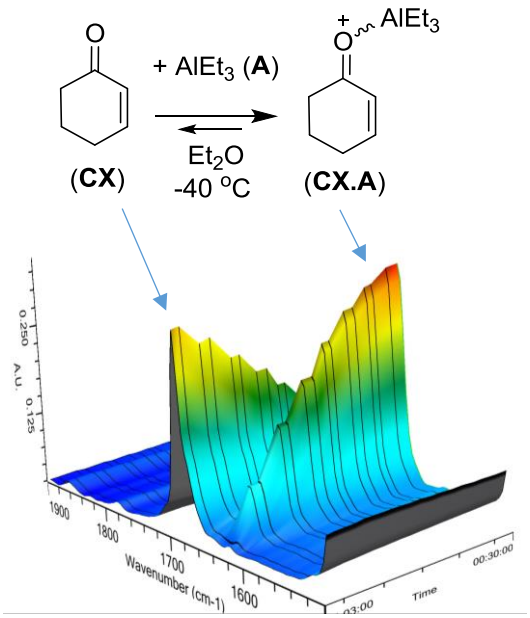

Figure 1. Formation of **CX**·**A** from **CX** and **A** (titrated in at *ca*. 0.1 equiv. steps) in Et_2O at -40 °C. Complexation is complete within the time of mixing (<5 sec) and provides K = 12.0(8) M^{-1}. The values in parentheses indicate the standard deviation in the last digit based on linear correlations of R^2 >0.99 for all fitted data.

Further credence to the proposal of Figure 1 is given by simple DFT modelling at the CAM-B3LYP/6-31G(d,p) level (Supporting Information). The calculated ΔG^{o}_{react} values for exchange of $Et_3Al{\cdot}OEt_2$ (the expected $AlEt_3$ speciation in Et_2O at -40 °C) with **CX** to provide the *syn* or *anti* isomers of **CX.A** are -6.4 and -6.1 kcal mol^{-1} respectively. This is broadly in line with the experimentally observed free energy. These simple (gas phase) calculations overestimate ΔG^{o}_{react} as the effect of solvation is ignored. The presence of an Et_2O solvent cage around **CX.A** is expected to favour back reaction to **A**.OEt_2. Similarly, the predicted ratio of the carbonyl stretching frequencies $\nu(C{=}O)_{\mathbf{CX}}/\nu(C{=}O)_{\mathbf{CX.A}}$ for both *syn*/*anti*-**CX.A** vs. **CX** are calculated at ~1.05 [CAM-B3LYP/6-31G(d,p)], compared to the experimental ratio of 1.03 (1676/1630 cm^{-1}).

Catalyst order in CX.A. The reaction order of Scheme 2 in **CX.A** is formally attained from the slope of plots of $\ln(k_{obs})$ as a function of $\ln[\mathbf{CX.A}]_0$ for the catalytic reaction at time t = 0. The adduct's initial concentration $[\mathbf{CX.A}]_0$ can be calculated from the known added $[\mathbf{CX}]_0$ and $[\mathbf{A}]_0$ via K = 12.0(8) M^{-1} (Eq 8, Supporting Information). Preliminary monitoring of a standard $Cu(OAc)_2$ (**Cu**) catalysed (3.0 mM, 1 mol-%) reaction using (*R,S,S*)-Feringa ligand (**L**) (4.5 mM, 1.5 mol-%) using **CX** (0.35 M) and **A** (0.39 M, 1.2 equiv) reveal the presence of an induction period in the first ca. 200-300 sec (Figure 2). This was most clearly demonstrated by the rise of product ee_P as a function of time[17] and the maximum seen early on in the absorbance ($O_{CX.A}$) of species **CX.A**. The induction period is not associated with formation of Cu^{I} as the $Cu(OAc)_2$/**L** mixture had already been cleanly reduced by prior treatment with $AlEt_3$ (125 eq, 10 min -40 °C)[15] prior to initiating the kinetic run by addition of **CX**. The homogeneous copper(I) pre-catalyst generated by pre-reduction is also stable under these conditions in this timeframe.[16]

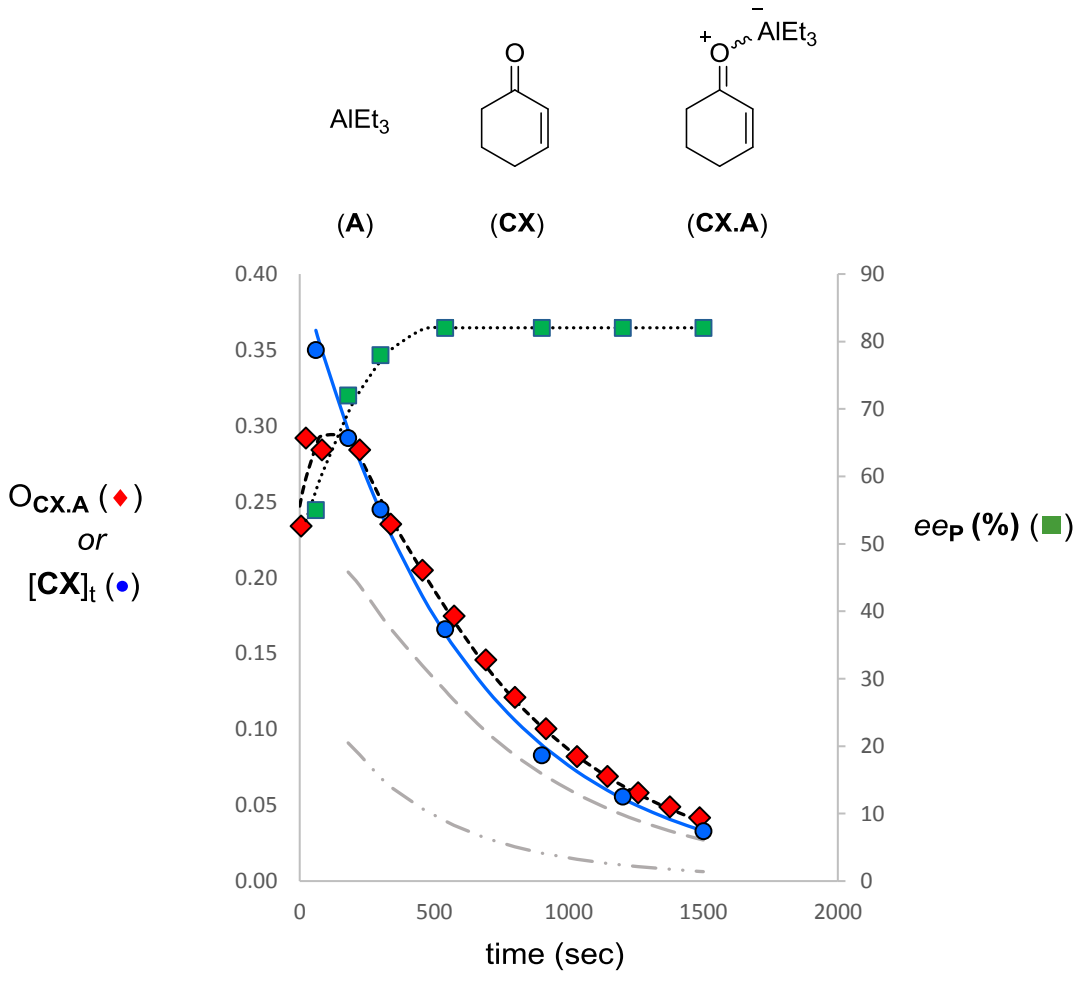

Figure 2. Representative monitoring of pre-reduced $Cu(OAc)_2$/**L** (1/1.5 mol-%) catalysed 1,4-addition of $AlEt_3$ (**A**, 0.35 M) to cyclohex-2-en-1-one (**CX**, 0.39 M) at -40 °C. Disappearance of **CX.A** was monitored via the intensity of its 1630 cm^{-1} IR stretch. Consumption of **CX** and the enantiomeric excess of the resultant product ee_P were determined by Krause's cryogenic sampling method[17] via subsequent chiral GC assay (Lipodex A). Key: observed absorbance ($O_{CX.A}$) of **CX.A** (◆) via ReactIR; concentration **CX** (●) and enantiomeric excess of product **P** (■) via chiral GC. The grey lines show calculated $AlEt_3$ bound cyclohex-2-en-1-one species $[\mathbf{CX.A}]_{t,calc}$ (– –) and free cyclohex-2-en-1-one $[\mathbf{CX}]_{t,calc}$ (– ··). The solid line (—) confirms the correlation $[\mathbf{CX}_{TOT}]_t$ = free $[\mathbf{CX}]_t$ + $[\mathbf{CX.A}]_t$ detected in the GC experiments. For derivations see Figure S3 in Supporting Information).

In the induction period (0-300 sec) catalyst genesis and immediate subsequent catalytic cyclohex-2-en-1-one (**CX**) turnover compete; beyond it catalysis is clearly dominated by a single copper species that provides the product (**P**) in ~82% *ee*. Post induction, the disappearance of [**CX**] and [**CX.A**] both fit first order behaviour best (R^2 = 0.98-0.99+)[18] and correlation of the ReactIR and GC monitoring can be shown by their data interconversion (Figure 2 above and S3 in Supporting Information) within experimental error. By fitting $O_{CX.A}$(1630 cm^{-1}) to [**CX.A**] beyond 300 sec using $[\mathbf{CX.A}]_0\exp(-k_1t)$ the induction period can thus be mathematically eliminated (Runs 3-6). In these trials the **Cu**:**L** ratio was kept fixed at 1:1.5 (±0.05) with nominal $[\mathbf{Cu}]_0$ = 3.5, $[\mathbf{L}]_0$ = 5 mM and with $[\mathbf{CX.A}]_0$ in the range 40-300 mM. The desired $\ln([\mathbf{CX.A}]_0)$ vs. $\ln(k_1)$ plot provided a best fit slope of 1.0 (Figure S4) commensurate with the enantioselective catalytic reaction being first order in **CX.A**.[18] In practice, due to the presence of the induction period and experimental off-sets in $O_{CX.A}$ it was easier to study change in [**CX.A**] as this leads directly to k_1 (which are independent of the measured $[\mathbf{CX.A}]_0$, avoiding tedious calibration of the crude absorbance (typically the value of $A_{obs,0}$ was ~0.35), and also avoiding repetitive checking of experimental off-sets in absorbance).

Catalyst order in Cu. Pre-reduction of $Cu(OAc)_2$ with $AlEt_3$ in the presence of **L** leads to quantitative formation of a stable Cu^I pre-catalyst with concentration [**Cu**].[16] By keeping a constant **Cu**:**L** ratio of 1:1.5 (±0.05) and varying the $[\mathbf{Cu}]_0$ concentration 1-6 mM at constant $[\mathbf{CX.A}]_0$ of 220 mM the order of the enantioselective reaction in copper(I) (**Cu**) could be determined. Reactions were monitored by ReactIR using post induction period decay data from $O_{CX.A}$ (Runs 7-10, Supporting Information). Data from these trials were fitted to $[\mathbf{CX.A}]_0\exp(-k_1t)$. A $\ln([\mathbf{CX.A}]_0)$ vs. $\ln(k_1)$ plot provided a best fit slope of 1.5 (Figure S5, Supporting Information) indicating that, post induction period, the enantioselective catalytic reaction is best described by a $[\mathbf{Cu}]^{1.5}$ order term.

Catalyst order in L. At fixed copper concentration (3.5 mM) the rate of the catalytic reaction shows both ligand acceleration and ligand retardation regions. Initial $\ln[\mathbf{L_0}]$ vs. $\ln(k_1)$, where the k_1 was derived from the first order decay of $O_{CX.A}$ for the species **CX.A**, gives a ligand acceleration order of 0.67 for regimes $0.5 \leq [\mathbf{L}]/[\mathbf{Cu}] \leq 3.5$ (Figure 3). For ligand concentrations where $[\mathbf{L}]/[\mathbf{Cu}] \geq 3.5$ transition to zero order kinetics is observed providing an inhibition order of -2.5 in ligand (Figure 3 and Figures S6-S7). As these ligand orders provide critical pointers to the **Cu**:**L** ratio in the transition state leading to asymmetric C—C bond formation they were also determined by GC study of $[\mathbf{CX}]_t$ (see Supporting Information). The average of three separate analyses across both GC and ReactIR data gave ligand reaction orders of 0.66 and -2.52 for the separate ligand acceleration and retardation processes respectively (Runs 9 and 11-23, Supporting Information). The only difference detected between the ReactIR and GC studies was that the greater data density of the former allowed the detection that the retardation process fits better to zero order, rather than first order, kinetics.

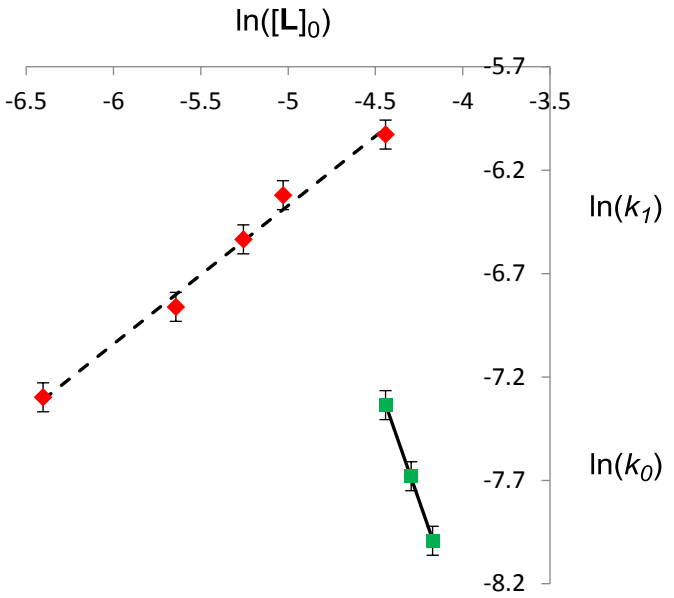

Figure 3. ReactIR ligand (**L**) order plot for catalysis of Scheme 1 showing both acceleration (rate ∝ [**L**]$^{0.67(4)}$) and deceleration (rate ∝ [**L**]$^{-2.42(5)}$) regions for [**Cu**] = 3.5 mM (1 mol-%). The values in parentheses, indicate the standard deviation in the last digit based on linear correlations of R^2 >0.99 for all fitted data (◆ k_1, first order for ligand acceleration; ■ k_0, zero order for ligand deceleration).

Data attained from the ReactIR kinetic studies of the dependence on **CX.A**, **Cu** and **L** are collected together in Table 1.

Table 1. Summary of the ReactIR investigations carried out in this study.

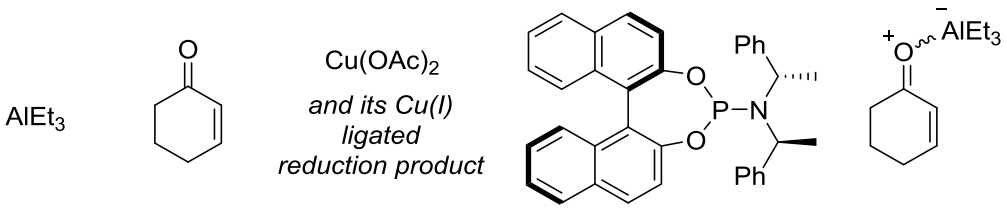

(**A**) (**CX**) (**Cu**) (**L**) (**CX.A**)

Run	[**A**]$_0$ (mM)	[**CX**]$_0$ (mM)	[**Cu**]$_0$ (mM)	[**L**]$_0$ (mM)	[**CX.A**]$_0$ (mM)	[**L**]$_0$/[**Cu**]$_0$	k_1 ×10^3 (s^{-1})[a]
1	0-340	337-406	-	-	0-207	-	-
2	0-345	421-481	-	-	0-237	-	-
3	520	413	3.46	4.99	300	1.44	1.558(8)
4	402	345	3.18	4.88	232	1.54	1.94(3)
5	255	202	3.55	5.22	124	1.47	0.566(7)
6	125	80.1	3.13	4.76	40.4	1.52	0.240(4)
7	397	337	1.07	1.59	226	1.49	0.323(4)
8	381	327	1.96	3.06	217	1.55	0.490(5)
9	379	321	3.79	5.49	213	1.45	1.517(9)
10	380	311	6.10	8.82	218	1.45	4.33(9)
11	396	351	3.62	1.66	232	0.46	0.674(4)
12	403	397	3.55	3.54	254	1.00	1.066(5)
13	396	339	3.19	6.54	227	2.05	1.94(2)
14	408	332	3.36	11.7	227	3.54	2.76(3)[b]
15	428	362	3.35	13.6	248	4.07	2.60(6)[b]
16	386	330	3.42	15.4	220	4.51	1.63(3)[b]

[a] For consumption of **CX.A**, a value of 1.558(8) equates to 1.558(8) × 10^{-3} s^{-1}. [b] First order fit given to allow direct comparison with other Table 1 data; the zero order (k_0) rate constants attained for runs 14-16 in Figure 3 are respectively: 4.56(6) × 10^{-4} M s^{-1}, 3.24(3) × 10^{-4} M s^{-1} and 2.35(2) × 10^{-4} M s^{-1}.

■ DISCUSSION

The presence of competing catalyst genesis followed by turnover in its early stages made the chemistry of Scheme 2 more suited to classical reaction order investigations rather than reaction progression analysis,[19] in our hands at least. Formation of the active catalyst for Scheme 2 is not associated with $Cu(OAc)_2$ reduction as a pre-reduction protocol is used prior to turnover initiation by **CX** addition. A similar catalyst induction period was also noted, but discounted, in Noyori's original rate studies of sulphonamide 1,4-addition catalysts – even though in this case no reduction is possible as Cu^I sources were used from the outset.[8] The possibility that the enolate species (**E**), formed in the initial induction period might be involved in the formation of a more active and selective catalyst was also not considered at that time. Post induction period, our ligand accelerated copper-catalysed 1,4-addition of $AlEt_3$ to cyclohex-2-en-1-one shows a rate law ∝ [**CX.A**]^1[**Cu**]$^{1.5}$[**L**]$^{0.66}$. One simple transition state stoichiometry deducible from this rate law is twice this: Cu_3**L**$_{1+x}$**CX**$_2$**A**$_2$ (x ~ 0.33) This is not in line with behaviour analogous to complexes **4-6** being involved as, in the simplest analysis, these would imply transition state stoichiometries of: Cu**LCXA** (Grignard), Cu**LCXA**$_2$ (organozinc) or Cu_2**L**$_3$**CXA** (NMR proposal) respectively. In their solution model studies[9] Gschwind and co-workers also detected an alternative to their dimeric [**L**$_2$Cu(μ-Cl)$_2$Cu**L**] pre-catalysts which was the trigonal complex [Cu(μ-Cl)**L**]$_3$. This form is (depending on reaction conditions) nearly isoenergetic with the dimer and favoured by lower **L**/Cu ratios and ethereal-based solvent systems. Structures based on (Cu**L**)$_3$ were originally argued against, in favour of Cu_2**L**$_3$, on the basis that catalyst stereoselectivity in $ZnEt_2$ 1,4-addition was maximised at **L**/Cu = 1.5 for zinc-based additions.[9,20] This is not the case in the aluminum catalysis of Scheme 2 where the product *ee* remains high (82%) down to **L**/Cu = 0.45 rather supporting a Cu_3:**L**$_{1.3}$ ratio in events leading up to and including the rate determining step.

Mechanistic proposal. Any mechanistic proposal, for the asymmetric 1,4-$AlEt_3$ addition catalysed by Cu^I/**L** studied here, has to account for the presence of the observed induction period and the inhibition seen at high phosphoramidite **L** (relative to Cu) concentrations where rate ∝ [**L**]$^{-2.5}$. One hypothesis consistent with these requirements, and the observed reagent orders, is shown in Scheme 3. The transition state (**7**) allows rapid interconversion between two C_2 related equivalent intermediates (**8**). Each catalytic turnover (**8** → **7** → C_2-**8**) results in clean interconversion of copper sites Cu_A and Cu_B. In the early stages of the reaction as no enolate (**E**) is available the concentration of **7** is limited and an induction period results. In the presence of excess ligand off-cycle inhibition is observed via **9**. Regeneration of **8** from **9** is expected to be zero order in **L** at high [**L**], as observed. We note that the Cu(μ-alkyl)Cu mode proposed for **9** was recently detected crystallographically for a methyl unit.[21] The stoichiometry of **7** [Cu_3**L**$_2$**CX**$_2$**A**$_2$] is in accord with twice the observed rate law ([**CX.A**]^1[**Cu**]$^{1.5}$[**L**]$^{0.66}$), through the molecularity **E** = **CX**+**A**.[22,23] As only the ligand **L** proximal to the catalytic site affects the conjugate addition rate only this fraction is detected in the kinetic studies; the other Cu**L** units plays only a structural role.[22] One explanation for how the Cu_3**L**$_2$ unit provides a ligand molecularity of [**L**]$^{1.33}$ through rapid ligand exchange is shown in Scheme 4. The structure of **8** was confirmed in DFT model studies (**8'** using the ωB97X-D[23] functional and Stuttgart-Bonn pseudopotential and basis set for Cu[24], with the 6-311G(d) basis set[25] for all other atoms, see Supporting Information) using a simplified ligand set, which nevertheless indicated the proposed Cu-Et…Al distal contact (C…Al 4.14 Å, see Supporting Information). Model intermediate **8'** readily coordinated an additional molecule of **CX.A** and this rapidly evolves towards model species closely related to **7** in line with the observed molecularity.

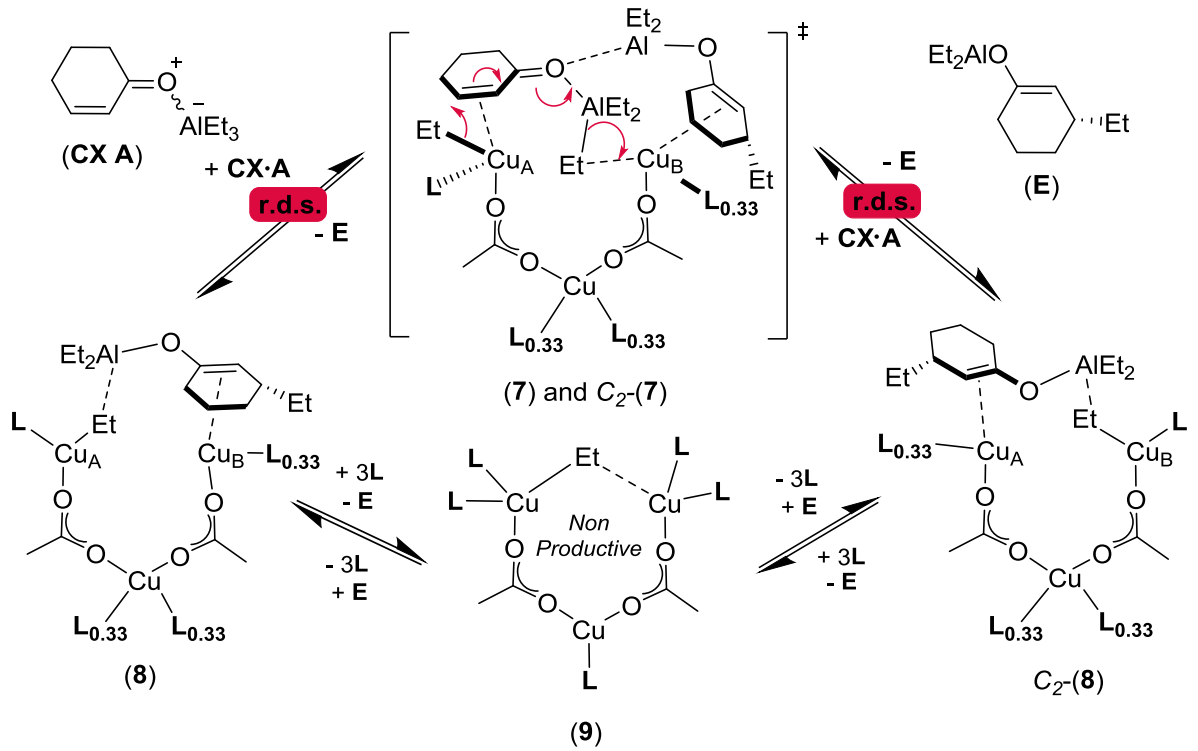

Scheme 3. Mechanism for Cu^{I}/**L** 1,4-addition of $AlEt_3$ (**A**) to cyclohex-2-en-1-one (**CX**) consistent with all experimentally observed data herein. The presence of any metal-coordinated solvent is excluded for clarity; $\mathbf{L}_{0.33}$ indicates partial (33%) binding to that site.[22] Each catalytic cycle interconverts Cu_A with Cu_B and their respective roles within the cycle.

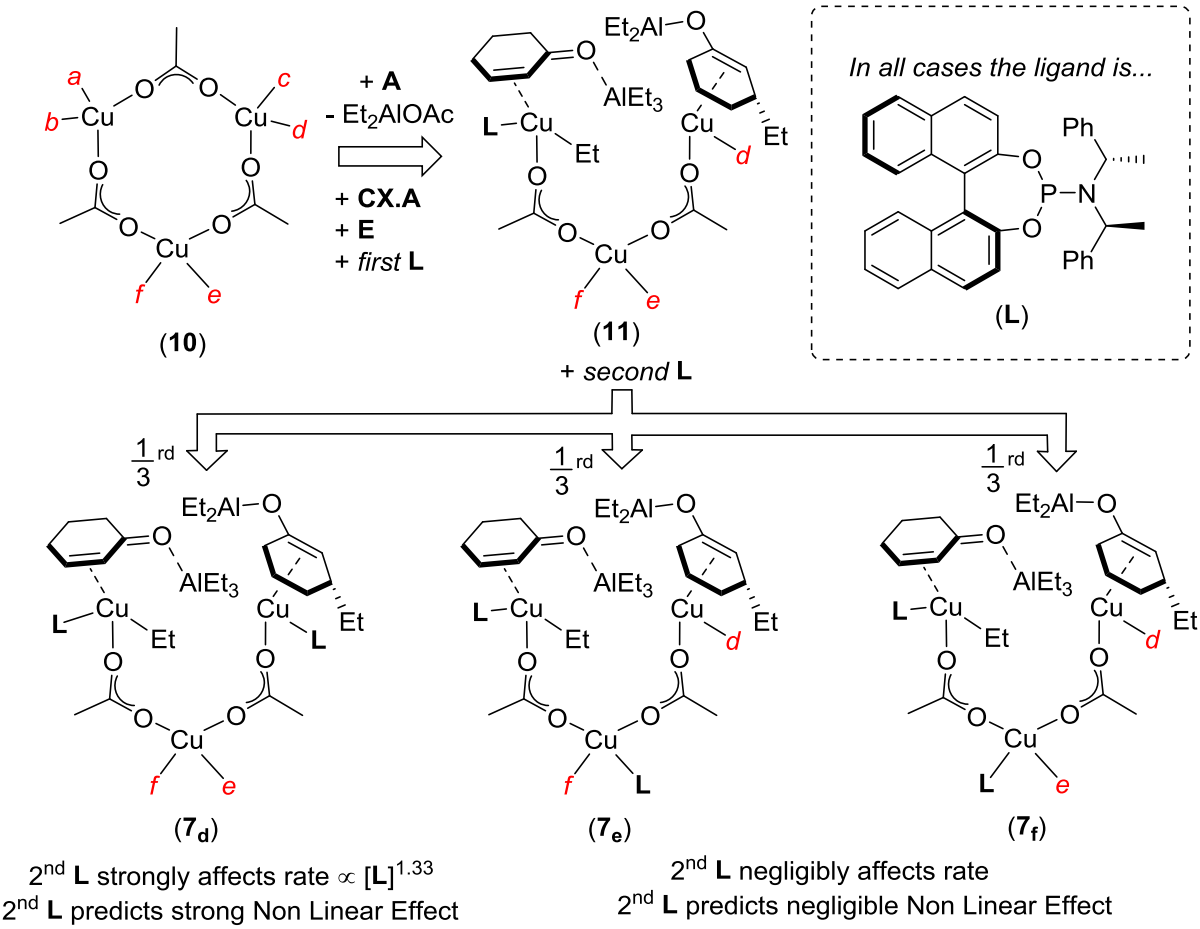

Scheme 4. Origin of the 1.33 ligand (**L**) molecularity. Trigonal $Cu_3(OAc)_3$ (**10**) has six additional ligand coordination sites (a-f). Loading this with **A**, **CX.A**, **E** and *one* **L** provides structure (**11**) with three remaining coordination sites (d-f). The *second* **L** loads randomly into these sites. Formation of **7d** leads to the 'shuttling mechanism' of Scheme 3 and the observed $[\mathbf{L}]^{1.33}$ order.

The alternative transition state (**12**) to **7** was also considered (Scheme 5). It is kinetically indistinguishable from (**7**) but the experimental data for the induction period are not consistent with its presence. Our pre-reduction protocol leads to very rapid catalyst formation from fully homogeneous precursor solutions. While deliberately perturbing these conditions to favour non homogeneous systems did result in slower inductions no product formation was seen in these initial periods. Once fully dissolved, similar reaction rates to those normally observed operated. This suggests that dissolution effects are not the source of the induction. More importantly, if on completion of the catalytic reaction (Scheme 2, but before quenching) the mixture is re-dosed with further **CX** and **A**, catalysis restarts immediately, without any induction period, and with slightly increased enantioselectivity (3-4% higher than that of the initial run). This effect is rather supportive of the product **E** being ligated within the selective transition state. While we cannot completely discount **12** the overall data strongly support **7** being the major contributor.

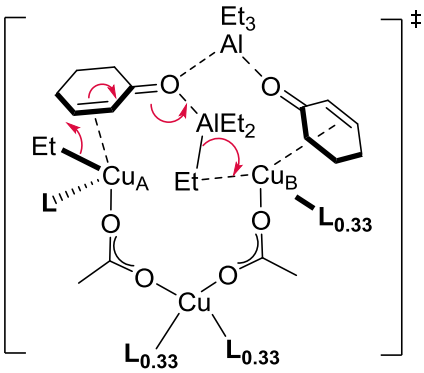

(**12**)

Scheme 5. Discounted alternative transition state to (**7**).

The presence of a $Cu_3\mathbf{L}_2$ stoichiometry in **7** predicts that the proximal $Cu_A\mathbf{L}$ and $Cu_B\mathbf{L}$ should lead to diasteriomeric transition states if less than 100% *ee* **L** is used. The proximity of these two ligands in intermediates leading to the rate determining (**7d**) dictates that such a system is expected to show a Non Linear Effect (NLE).[26] The enantiopurity of the ligand (**L**) was varied from 0-100% *ee* and a small positive NLE is experimentally observed when the *ee* of **L** is below ca. 50% (Runs 24-28, Table S1, Supporting Information). These experimental data are well simulated by our kinetic model whereby the homochiral catalyst ($\mathbf{L}_R$,$\mathbf{L}_R$) provides (*R*)-3-ethylcyclohexanone (**P**) in 82% *ee* and the heterochiral catalyst ($\mathbf{L}_R$,$\mathbf{L}_S$) leads to the same enantiomer of product **P** in 99% *ee*, but this is formed 1.4 times slower than the homochiral catalyst (Figures S7-S8, Supporting Information).

■ CONCLUSIONS

Gschwind's hypothesis, that a single dominant copper/phosphoramidite species is responsible for the ACA reactions of 'softer' organometallics, is supported by the studies herein. However, our data are most in accord with the major chemical entity responsible for the catalytic 1,4-addition of $AlEt_3$ to cyclohex-2-en-1-one being a $Cu_3\mathbf{L}_2$ trimer rather than the $Cu_2\mathbf{L}_3$ dimer proposed for analogous zinc chemistry. A catalytic cycle involving shuttling between two C_2-symmetry related ground states (**8**) each containing a π-bound enolate and a Cu-Et bond is an attractive proposal, in that: (i) it leads to a transition state stoichometry in line with a simple interpretation of the primary kinetic data; (ii) the $-OAlEt_2$ Lewis acid function of the Cu π-bound enolate offers a favourable additional point of binding and activation for the cyclohex-2-en-1-one/$AlEt_3$ adduct (**CX·A**) as this docks into the catalyst; (iii) the conjugate addition triggers both formation and expulsion of the enolate product (**E**) facilitating fast turnover; (iv) it explains the

experimentally observed induction period; (v) it offers a prediction of the observed NLE; (vi) the proposed r.d.s. stoichiometry correlates well with older observations that stoichiometric cuprates typically require 2:1 ratios of MR:CuX before they become active in additions to enones;[27] finally (vii) simple DFT computational models are also in accord with the proposal. While the real catalytic mixture undoubtedly contains small populations of other species the data attained here are most in accord with the major catalytic reaction manifold occurring via the cycle of Scheme 3. The presence of a bound enolate (**E**) within the selective transition state of the 1,4-conjugate addition catalyst is a key finding of this present study. Enolate-catalyst incorporation provides an insight in to a long observed, but previously non explained fact: in copper-catalysed ACA reactions of organoaluminum species the most active and selective catalysts are frequently realised from very labile copper(I) sources, such as $[Cu(MeCN)_4]BF_4$, it is these species that are of course most predisposed to product enolate incorporation.

■ AUTHOR INFORMATION

Corresponding Author
*E-mail: simon.woodward@nottingham.ac.uk
ORCID
Simon Woodward: 0000-0001-8539-6232
Notes
The authors declare no competing financial interest.

■ ASSOCIATED CONTENT

Supporting Information
The Supporting Information is available free of charge on the ACS Publications website at:
XXeditorial office to insertXX.

Experimental procedures, derivation of binding isotherms, and primary data for all Runs (1-28).

Final calculated coordinates for intermediates (*syn/anti*-**CX.A** and models **8'** and **8'-CX.A**).

■ ACKNOWLEDGMENTS

SW is grateful to the Engineering and Physical Sciences Research Council (EPSRC) for access to national service for computational chemistry (NSCCS) for computational facilities until their closure in 2017 and for provision of a CASE studentship to AK (in collaboration with Key Organics Ltd, award reference 1507028). RN and DW thank the University of Nottingham for studentships and access to ReactIR facilities. This study was also facilitated by a donation from Aesica pharmaceuticals Ltd (Cramlington, UK).

■ REFERENCES

(1) General overviews of ACA reactions see: (a) *Copper-Catalyzed Asymmetric Synthesis*; Alexakis, A., Krause, N., Woodward, S. Eds.; Wiley-VCH: Weinheim, 2014. (b) Thaler, T.; Knochel, P. *Angew. Chem. Int. Ed.* **2009**, *48*, 645-648. (c) Alexakis, A.; Bäckvall, J.E.; Krause, N.; Pàmies, O.; Diéguez, M. *Chem. Rev*. **2008**, *108*, 2796-2823. (d) Falciola, C. A.; Alexakis, A. *Eur. J. Org. Chem*. **2008**, 3765-3780. For listings of early developments see: (e) Krause, N.; Hoffmann-Röder, A. *Synthesis* **2001**, 171-196.

(2) Ligand effects in ACA reactions: (a) Alexakis, A.; Krause, N.; Woodward, S. Copper-Catalyzed Asymmetric Conjugate Addition. In *Copper-Catalyzed Asymmetric Synthesis*; Alexakis, A., Krause, N., Woodward, S. Eds.; Wiley-VCH: Weinheim, 2014, pp 33-68 (also covers nucleophile and substrate types). (b) Minnaard, A. J.; Feringa, B. L. *Acc. Chem. Res*. **2007**, *40*, 179-188 (phosphoramidites). (c) Harutyunyan, S. R.; den Hartog, T.; Geurts, K.; Minnaard, A. J.; Feringa, B. L. *Chem. Rev*. **2008**, *108*, 2824-2852 (diphosphines, especially Josiphos). (d) Hajra, A.; Yoshikai, N.; Nakamura, E. *Org. Lett*. **2006**, *8*, 4153-4155 (mixed *P,O*-donors). (e) Germain, N.; Magrez, M.; Kehrli, S.;Mauduit, M.; Alexakis, A. *Eur. J. Org. Chem*. **2012**, 5301-5306 (NHC ligands). (f) Palais, L.; Alexakis, A. *Chem. Eur. J.* **2009**, *15*, 10473-10485 (simplephos).

(3) Reviews of mechanistic aspects: (a) N. Yoshikai, N.; Nakamura, E. *Chem. Rev*. **2012**, *112*, 2339-2372. (b) Woodward, S. and Willcox, D. Ligated Organocuprates: An A-Z

Routemap of Mechanism and Application. In *Innovative Catalysis in Organic Synthesis*; Andersson, P. G. Ed.; Wiley-VCH, Weinheim 2012, pp 233-255. (c) Jerphagon, T., Pizzuti, M. G., Minnaard, A. J., Feringa, B. L. *Chem. Soc. Rev.* **2009**, *38*, 1039-1075 (d) Rovis, T., Evans, D.A. *Prog. Inorg. Chem*. **2002**, *50*, 1-150. (e) Nakamura E., Mori S. *Angew. Chem. Int. Ed.* **2000**, *39*, 3750-3771. (f) Gallo, E.; Ragaini, F.; Bilello, L.; Cenini, S.; Gennari, C.; Piarulli, U. *J. Organomet. Chem*. **2004**, *689*, 2169-2176. (g) Bertz, S. H.; Cope, S.; Murphy, M.; Ogle, C. A.; Taylor, B. J. *J. Am. Chem. Soc*., **2007**, *129*, 7208-7209. For a summary of early work see: (h) Mori, S., Nakamura, E. Mechanisms of Copper-mediated Addition and Substitution Reactions. In *Modern Organocopper Chemistry*; Krause, N. Ed. Wiley-VCH: Weinheim 2002, pp 315-346. (i) den Hartog, T.; Huang, Y.; Fañanás-Mastral, M.; Meuwese, A.; Rudolph, A.; Pérez, M.; Minnaard, A. J.; Feringa, B. L. *ACS Catalysis* **2015**, *5*, 560-574.

(4) Characterised examples of π-complexes: (a) Bertz, S. H.; Hardin, R. A.;Heavey, T. J.; Ogle, C. A. *Angew. Chem. Int. Ed*. **2013**, *52*, 10250-10252 (by X-ray). (b) Uerdingen, M.; Krause, N.; *Tetrahedron* **2000**, *56*, 2799–2804 (by ^{13}C NMR). (c) Krause, N.; Wagner, R.; Gerold, A. *J. Am. Chem. Soc*. **1994**, *116*, 381-382 (by ^{13}C NMR).

(5) Copper(III) intermediates (detection method, geometry): (a) Chang, H.-C.; Lo, F.-C.; Liu, W.-C.; Lin, T.-H.; Liaw, W.-F.; Kuo, T.-S.; Lee, W.-Z. *Inorg, Chem*. **2015**, *54*, 5527-5533 (X-ray, tbp). (b) Hannigan, S. F.; Lum, J. S.; Bacon, J. W.; Moore, C.; Golen, J. A.; Rheingold, A. L.; Doerrer, L. H. *Organometallics* **2013**, *32*, 3429-3436 (X-ray, square planar). (c) Bertz, S. H.; Hardin, R. A.; Murphy, M. D.; Ogle, C. A.; Richter, J. D.; Thomas, A. A. *J. Am. Chem. Soc*., **2012**, *134*, 9557-9560 (NMR, trigonal π-allyl). (d) Casitas, A.; King, A. E.; Parella, T.; Costas, M.; Stahl, S. S.; Ribas, X. *Chem. Sci*. **2010**, *1*, 326-330 (X-ray, square based pyramidal). (e) Bartholomew, E. R.; Bertz, S. H.; Cope, S. K.; Murphy, M. D.; Ogle, C. A.; Thomas, A. A. *Chem. Commun*. **2010**, *46*, 1253-1254 (NMR, square planar). (f) Bertz, S. H.; Murphy, M. D.; Ogle, C. A.; Thomas, A. A. *Chem. Commun*. **2010**, *46*, 1255-1256 (NMR, square planar). (g) Bartholomew, E. R.; Bertz, S. H.; Cope, S.; Dorton, D. C.; Murphy, M.; Ogle, C. A. *Chem. Commun*. **2008**, 1176-1177 (NMR, square planar, ligated). (h) Bertz, S. H.; Cope, S.; Murphy, M.; Ogle, C. A.; Taylor, B. J. *J. Am. Chem. Soc*. **2007**, *129*, 7208-7209 (NMR, square planar). For an introductory overview of this area see: (i) Bertz, S. H.; Cope, S.; Dorton, D.; Murphy, M.; Ogle, C. A. *Angew. Chem. Int. Ed.* **2007**, *46*, 7082-7085.

(6) Harutyunyan, S.R.; López, F.; Browne, W. R.; Correa, A.; Peňa, D.; Badorrey, R., Meetsma, A., Minnaard, A. J., Feringa, B. L. *J. Am. Chem. Soc*. **2006**, *128*, 9103-9118.

(7) Pfretzschner, T.; Kleemann, L.; Janza, B.; Harms, K.; Schrader, T. *Chem. Eur. J.* **2014**, *10*, 6048-6057.

(8) Kitamura, M.; Miki, T.; Nakano, K.; Noyori, R. *Bull. Chem. Soc. Japan* **2000**, *73*, 999-1014. These workers attributed their induction period to catalyst dissolution effects.

(9) (a) Zhang, H.; Gschwind, R. M. *Angew. Chem. Int. Ed.* **2006**, *45*, 6391-6394. (b) Zhang, H.; Gschwind, R.M. *Chem. Eur. J.* **2007**, *13*, 6691-6700. (c) Schober, K.; Zhang, H.; Gschwind, R. M. *J. Am. Chem. Soc.* **2008**, *130*, 12310-12317. (d) von Rekowski, F.; Koch, C.; Gschwind, R. M. *J. Am. Chem. Soc*. **2014**, *136*, 11389-11395. For an overview of NMR applications in cuprate catalysis see: (e) von Rekowski, F.; Koch, C.; Gschwind, R. M. NMR Spectroscopic Aspects. In *Copper-Catalyzed Asymmetric Synthesis*; Alexakis, A., Krause, N., Woodward, S. Eds.; Wiley-VCH: Weinheim, 2014, pp 353-372. (f) R. M. Gschwind, *Chem. Rev*. **2008**, *108*, 3029-3053.

(10) Pàmies, O., Diéguez, M. Conjugate Addition of Organoaluminum Species to Michael Acceptors and Related Processes. In *Modern Organoaluminum Reagents*; Woodward, S., Dagorne, S. Eds.; Springer, New York, 2013, pp 277-306.

(11) Other options for catalytic asymmetric additions of alkyl nucleophiles to β,β-substituted enones exist, notably zirconium reagents, for recent examples see: (a) Gao, Z.; Fletcher, S. P. *Chem. Science* **2017**, *8*, 641-646. (b) Garrec K.; Fletcher, S. P. *Org. Lett*. **2016**, *18*, 3814-3817.

(12) The only rate study we can identify is an early qualitative correlation of [Cu] to initial rate for a ligandless system: Kabbara, J. Flemming, S.; Nickisch, K.; Neh, H.; Westermann, J. *Chem. Ber.* **1994**, 127, 1489-1493.

(13) The only related measurement we could identify was AlMe(2,6-tBu_2-4-$MeC_6H_2O)_2$ with benzophenone in toluene-d_8: K(35 °C) = 38.2 M^{-1}, ΔH_f^o = 67.1 kJ mol^{-1} (16.0 kcal mol^{-1}): (a) Power, M. B.; Nash, J. R.; Healy, M. D.; Barron, A. R. *Organometallics* **1992**, *11*,

1830-1840. A ketone complex of $AlEtCl_2$ has been identified by ^1H NMR spectroscopy but no binding (association) constant measured: (b) Childs, R. F.; Duffey, B. M.; Mahendran, M. *Can. J. Chem*. **1986**, *64*, 1220-1223.

(14) The presence of such R_3Al▪enone adducts has been widely assumed to be the reason for the enhanced activity of alanes in the formation of quaternary centres in ACA reactions (see: Alexakis, A.; Krause, N.; Woodward, S. Copper-Catalyzed Asymmetric Conjugate Addition. In *Copper-Catalyzed Asymmetric Synthesis*; Alexakis, A., Krause, N., Woodward, S. Eds.; Wiley-VCH: Weinheim, 2014, pp 33-68), but they had remained undetected.

(15) Reduction is rapid and complete under such conditions see: (a) Yan, M.; Yang, L.W.; Wong, K.Y.; Chan, A.S.C. *Chem. Commun*. **1999**, 11–12 [NMR study]. (b) See Pfretzschner, T.; Kleemann, L.; Janza, B.; Harms, K.; Schrader, T. *Chem. Eur. J.* **2014**, *10*, 6048-6057 for an EPR study. Pre-reduction to Cu^I before catalysis also avoids the potential for competing radical effects see: (c) Li, K.; Alexakis, A. *Angew. Chem. Int. Ed.* **2006**, *45*, 7600-7603.

(16) In fact in favourable examples these may be isolated: Mothes, R.; Ruffer, T.; Shen, Y.; Jakob, A.; Walfort, B.; Petzold, H.; Schulz, S. E.; Ecke, R.; Gessner, T.; Lang, H. *Dalton Trans.* **2010**, *39*, 11235-11247.

(17) For the technique used see: Canisius, J.; Gerold, A.; Krause, N. *Angew. Chem. Int. Ed*. **1999**, *38*, 1644-1646.

(18) The greater data density of the ReactIR studies allowed us to confidently discriminate between various empirical rate laws. Consistently better fits were attained to first order disappearance of **CX▪A** (vs. zero, second order, and first order near equal concentration) rate laws based on R^2 values. Consistent with this picture switch to zero order behaviour at high **L** concentrations was detected. For lower data dentist GC data points were fitted only to first order behaviour. See also Supporting Information.

(19) Blackmond D. G. *Angew. Chem. Int. Ed.* **2005**, *44*, 4302-4320.

(20) Alexakis, A; Benhaim, C. *Eur. J. Org. Chem*. **2002**, 3221-3236.

(21) Molteni, R.; Bertermann, R.; Edkins, K.; Steffen, A. *Chem. Commun*. **2016**, *52*, 5019-5022.

(22) An alternative model where each of the four coordination sites on the three coppers has an occupancy of 1/3 was also considered. This is mechanistically indistinguishable from Scheme 3-4. Phosphorus-31 NMR studies under reaction conditions identical to the kinetic studies show only a single ^{31}P signal (144.5 ppm) confirming ligand exchange. All such valid structures for **7** have the stoichiometry Cu_3**L**$_2$**CX▪A▪E**, equivalent to Cu_3**L**$_2$**CX**$_2$**A**$_2$ through the molecularity **E** = **CX** + **A**.

(23) Chai, J.-D.; Head-Gordon, M. *Phys. Chem. Chem. Phys.* **2008**, *10*, 6615-6620.

(24) Dolg, M.; Wedig, U.; Stoll, H.; Preuss, H. *J. Chem. Phys.* **1987**, *86*, 866-872.

(25) Krishnan, R.; Binkley, J. S.; Seeger, R.; Pople, J. A. *J. Chem. Phys.* **1980**, *72*, 650-654.

(26) Kagan, H. B.; Girard, C. *Angew. Chem. Int. Ed.* **1998**, *37*, 2922-2959.

(27) Alexakis, A.; Benhaim, C.; Rosset, S.; Humam, M. *J. Am. Chem. Soc.* **2002**, *124*, 5262-5263.

Graphic for Table of Contents